Radiological Imaging in Acute Lung Injury and Acute Respiratory Distress Syndrome

Pietro Caironi, M.D.,[1] Eleonora Carlesso, M.Sc.,[1] and Luciano Gattinoni, M.D., F.R.C.P.[1]

ABSTRACT

Computed tomography (CT) has been utilized to study acute respiratory distress syndrome (ARDS) since the middle 1980s, when it revealed the inhomogeneous pattern of the lung lesion. Its advantages rely on the strict correlation between CT density and the lung physical density, allowing a quantification of lung compartments with different degrees of aeration. By CT scans, ARDS lung appeared to be "small" rather than "stiff," leading to the "baby lung" concept. The regional analysis revealed that this appearance derives from an evenly distributed lung edema, which tends, because of gravitational forces, to lie predominantly in the most dependent regions, leading to alveolar collapse. New data suggest that such a "sponge lung" is made by a "core," consolidated, lung portion, from which, through an inflammatory reaction, lung edema will spread, determining the collapsed and recruitable lung portion. The amount of recruitable lung varies among ARDS patients. This knowledge is necessary for a rational positive end-expiratory pressure (PEEP) setting because the amount of tissue maintained aerated by PEEP is closely associated with the amount of recruitable lung. CT scans may also help to diagnose ARDS because CT provides a good estimate of the high-permeability lung edema, the characteristic lesion of this syndrome.

KEYWORDS: Acute respiratory distress syndrome, computed tomography, lung recruitment, positive end-expiratory pressure, mechanical ventilation

Medicine has always taken advantage, in approaching different diseases, of the possibility of looking inside the affected organ and visualizing the ongoing pathology. One of the main goals of laboratory research is to discover techniques that allow investigators to see pathological aberrations in affected organs. When acute respiratory distress syndrome (ARDS) was first described by Ashbaugh and colleagues,[1] the only available technique to visualize the pathological process in the lungs was conventional chest radiographs. Since the beginning, the presence of "bilateral alveolar infiltrates" was recognized as characterizing this syndrome, in association with marked hypoxemia and "stiffness" of the respiratory system, as judged by a very low compliance.[1,2] The invention of computed tomography (CT), and its application in ARDS patients since the middle 1980s,[3–5] provided the morphological and functional characterization of the injured lung that investigators and physicians had longed for. Chest CT revealed that ARDS was not a homogeneous process but rather an

[1]Istituto di Anestesiologia e Rianimazione, Dipartimento di Anestesia, Rianimazione, e Terapia del Dolore, Fondazione IRCCS–"Ospedale Maggiore Policlinico, Mangiagalli, Regina Elena" di Milano, Università degli Studi di Milano, Milano, Italy.

Address for correspondence and reprint requests: Luciano Gattinoni, M.D., Istituto di Anestesiologia e Rianimazione, Fondazione IRCCS–"Ospedale Maggiore Policlinico, Mangiagalli, Regina Elena" di Milano, Università, degli Studi di Milano, Via F. Sforza 35, 20122 Milano, Italy. E-mail: gattinon@policlinico.mi.it.

Acute Lung Injury and Acute Respiratory Distress Syndrome; Guest Editors, John A. Belperio, M.D., Michael A. Matthay, M.D., F.C.C.P.

Semin Respir Crit Care Med 2006;27:404–415.
DOI 10.1055/s-2006-948294. ISSN 1069-3424.

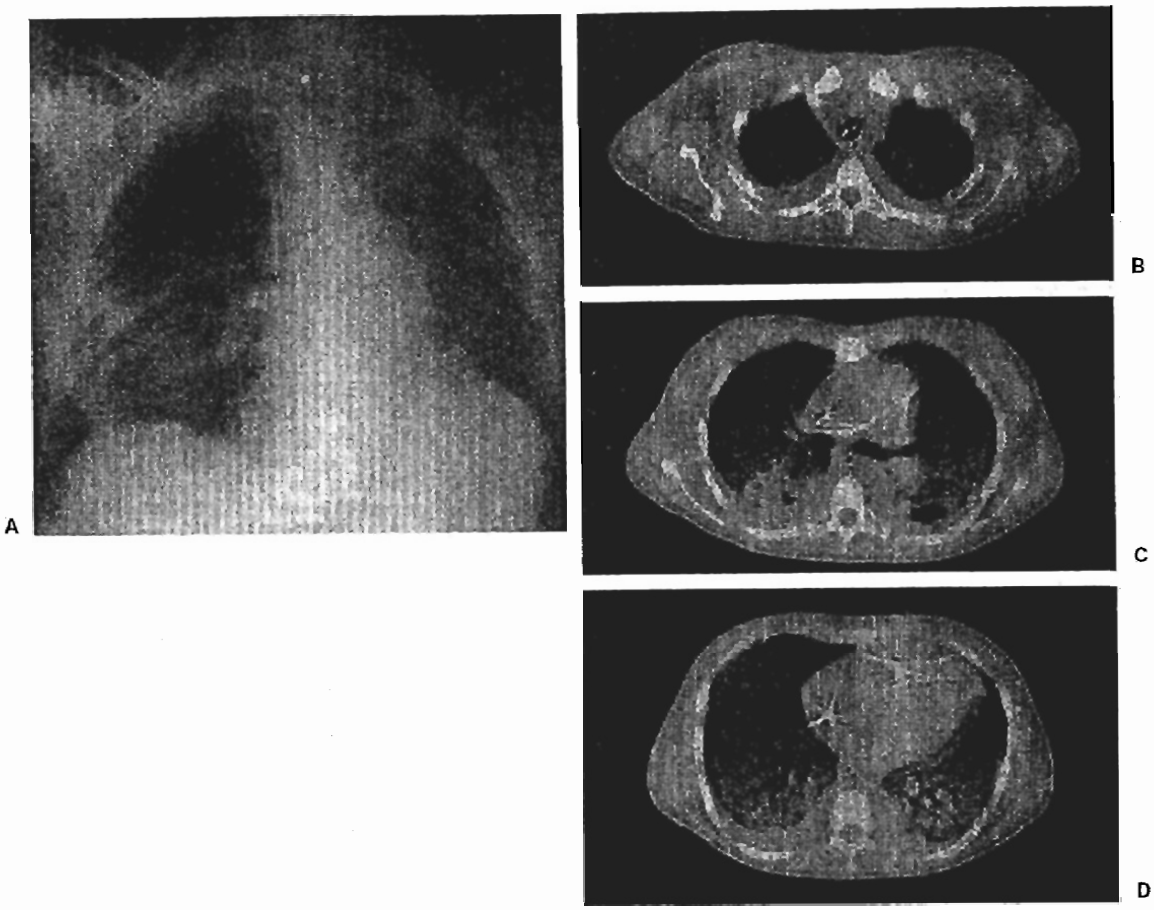

Figure 1 Anteroposterior chest x-ray (A), and corresponding lung computed tomographic (CT) scan images at apex, hilum, and base (B,C,D) of a patient affected by acute respiratory distress syndrome (ARDS) from sepsis. CT scanning was performed at end-expiration, at a positive end-expiratory pressure (PEEP) of 5 cm H_2O. Although the chest x-ray shows diffuse ground-glass opacification, sparing the right upper lung, the CT scans revealed an inhomogeneous disease, with both craniocaudal and sternovertebral gradients. From Gattinoni et al,[16] with permission.

uneven disease mainly affecting the most dependent lung regions[6] (Fig. 1). Chest CT scans are able to "quantify" the disease, expanding research applications. More recently, CT scans have been useful in examining myriad clinical issues, such as respiratory mechanics,[7–9] intra-abdominal pressure,[10] mechanical ventilation in dynamic conditions,[11,12] lung perfusion,[13,14] and lung recruitability.[15] This article reviews the cardinal findings and major applications of CT scans in the management of ARDS, with attention to the physical principles underlying its quantitative analysis.

QUANTITATIVE ANALYSIS OF CT SCAN IMAGES

The introduction of CT scan in the research and clinical treatment of ARDS patients has been a great success, especially in understanding the pathophysiology of the syndrome and the effects of some ventilatory variables usually set at the bedside.[16] Two main characteristics of CT scan, as compared with chest x-ray, contribute to its success: first, CT scans provide axial images of the lung parenchyma, thereby allowing a visualization of the inside portion of the lung; second, CT may "quantify" specific parameters obtained with images. But how do CT scans work?

Physical Principles of CT Scan Images

The mean feature that allows the use of CT scan images for a quantitative analysis relies on the numerical values associated to each unit in which the images are divided (i.e., the voxel), and that is represented by the CT number.[17] Indeed, this value represents the linear attenuation coefficient (μ) of x-ray beams through the matter; in other words, the reduction of the radiation intensity upon passage through the matter. When an x-ray beam arises from a radiation source, enters into matter, and emerges from it, it will be attenuated based upon each material encountered during the passage. The

CT number expresses the linear attenuation coefficient as referred to the one for water (the reference standard), according to the following formula:

$$CT = 1000 \times \left(\frac{\mu_{material} - \mu_{water}}{\mu_{water}} \right)$$

where $\mu_{material}$ represents the linear attenuation coefficient of the material analyzed, and μ_{water} represents the linear attenuation coefficient of water. To magnify the small difference of linear attenuation coefficients of different materials, a factor scale of 1000 is used. The process of attenuation of x-ray beams is based on some peculiar characteristics of this radiation. Because the wavelength of x-rays is very small ($\lambda = 10 - 10^{-3}$ Å), they usually penetrate into the matter more easily than longer electromagnetic waves; as a consequence, many different materials are almost transparent to them. An x-ray beam of initial intensity I_0, after having passed through a material of a given thickness x, will reach the detector with an intensity I that will be lower than the initial one because of the interaction with the atoms of the material passed through, according to the following formula:

$$I(x) = I_0 \times e^{-\mu x}$$

The linear attenuation coefficient μ shown above is actually the sum of the different linear attenuation coefficients determined by the different types of interactions of the x-ray beam and the material (photoelectric effect, Compton effect, and production of electron–positron pairs).

The importance and usefulness of the CT number, as here defined, rely on its strict association with the physical density (the ratio between mass and volume of a given material) of the material the x-ray beam has passed through with the CT scan. More precisely, the total linear attenuation coefficient is correlated to the physical density according to the following formula[18]:

$$\mu = \rho N_g \times [\sigma_R(Z_R, E) + \sigma_{P.e.}(Z_{P.e.}, E) + \sigma_c(E) + \sigma_\pi(Z_\pi, E)]$$

where Z denotes the atomic number for coherent interactions (Z_R), for interactions with photoelectric effect ($Z_{P.e.}$), and for interactions with the production of electron–positron pairs (Z_π); E denotes the energy of the incident photon; ρ the physical density (g/cm^3); Ng the density of electronic mass (electrons/g); σ_R the section that has been passed through, for each electron, by coherent interactions (cm^2/electrons); $\sigma_{P.e.}$ the section passed through, for each electron, with interactions for photoelectric effect (cm^2/electrons); σ_c the section passed through, for each electron, with interactions for Compton effect (cm^2/electron); σ_π the section passed through, for each electron, with the production of electron–positron pairs (cm^2/electron); and σ (Z, E) the section that has been passed through as a function of the atomic number Z and as a function of the energy of the incident photon E. Among all the types of electron interactions, the Compton effect contributes the most to the final x-ray attenuation.[19] Because all the variables affecting the x-ray attenuation are usually kept constant during CT scans in ARDS patients, it follows that a linear correlation between the "CT number," as detected on lung CT scan images, and physical density of the lung parenchyma can be reasonably assumed, as previously demonstrated in an experimental setting[6,17] (Fig. 2).

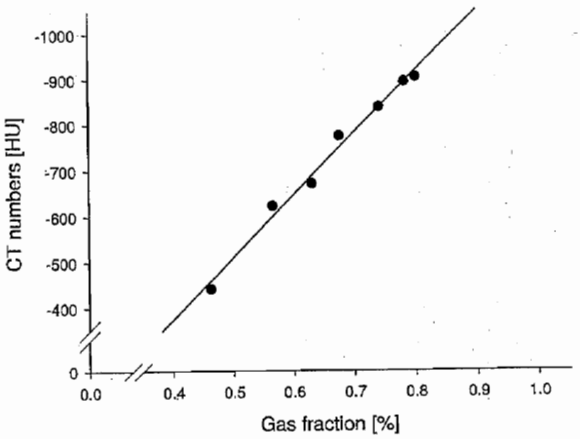

Figure 2 Pulmonary computed tomographic (CT) density as a function of the fractional gas content in isolated pig lungs. CT density is expressed in Hounsfield units, ranging, for the lung parenchyma, from −1000 HU to 0 HU. The fractional gas content denotes the fraction of lung volume that is filled with gas, expressed as a fraction between the gas volume and the total lung volume. As shown, the CT density strictly represents the physical density of the lung parenchyma ($r = 0.96$, $p < 0.01$). Modified from Gattinoni et al.[6]

The CT number or the CT physical density is measured in Hounsfield units (HU). The attenuation scale arbitrarily ranges from + 1000 HU, which approximates the physical density of bone (complete absorption), and −1000 HU, which approximates the physical density of air (complete transparency). Zero HU is approximately equivalent to the physical density of water. The lung tissue, which includes different anatomical entities, such as epithelial and endothelial cells, extravascular fluid, blood, fibrin, and others,[16] has a physical density very close to the one of water (1 g/mL or 0 HU). Consequently, the range of density we have to consider when dealing with the lung parenchyma is included between 0 HU and −1000 HU. If we consider the lung parenchyma as a mixture of two different types of material (i.e., air and tissue, including cells, blood, extravascular fluid, fibrin, etc.), it is possible to compute, for any given voxel of a lung CT image, the percentage of air and the percentage of lung tissue included in that specific volume of lung parenchyma. For example, a

voxel with a CT number of −700 HU will be characterized by 70% of air and 30% of lung tissue; in other words, 30% of its volume will be composed of cells, blood, and extravascular fluid, whereas 70% of its volume will be composed of gas.[20] In summary, the gas volume of a specific lung region of interest (ROI) may be computed as follows:

$$Gas\ volume_{ROI} = Total\ volume_{ROI} \times \left(\frac{mean\ CT_{ROI}}{-1000}\right)$$

where the $Total\ volume_{ROI}$ denotes the total volume of the specific lung area, and $mean\ CT_{ROI}$ denotes the mean density, expressed as the CT number, of the specific lung area. On the other hand, the amount of tissue included in a specific lung area may be computed as follows:

$$Tissue\ weight_{ROI} = Total\ volume_{ROI} \times \left[1 - \left(\frac{mean\ CT_{ROI}}{-1000}\right)\right]$$

or

$$Tissue\ weight_{ROI} = Total\ volume_{ROI} - Gas\ volume_{ROI}$$

where $Total\ volume_{ROI}$ denotes the total volume of the specific lung area, and $mean\ CT_{ROI}$ denotes the mean density, expressed as the CT number, of the specific lung area. Of note, the possibility of computing the tissue weight from a volume depends on the assumption that the physical density of the lung parenchyma is equal to that of water (1 g/mL).

Lung Compartment

To better investigate the morphology of the lung parenchyma and to evaluate its functionality in terms of gas exchange and variations according to different ventilatory settings, it is useful to examine and divide the lung parenchyma in different portions according to their degree of aeration.[20] Based on the frequency distribution of the CT numbers of an entire slice of lung CT scan in normal lungs, four different lung compartments can be easily recognized: (1) a nonaerated compartment, as defined by a CT number between −100 HU and +100 HU, which represents the portion of lung parenchyma that is gasless (i.e., collapsed, consolidated, or filled with extravascular fluid), together with a portion of lung parenchyma characterized by small airway collapse; (2) a poorly aerated compartment, as defined by a CT number between −101 HU and −500 HU; (3) a normally aerated compartment, as defined by a CT number between −501 HU and −900 HU, which represents the major lung compartment in healthy lung; (4) a hyperinflated compartment, as defined by a CT number between −901 HU and −1000 HU. The thresholds here reported for the different lung compartments are based on the normal distribution of CT numbers in healthy lungs.[20] Because slightly different thresholds have been proposed by other authors,[16] caution must be applied when comparing the findings reported by different groups of investigators.

The advantage of this approach may be easily understood. If we need to evaluate the efficacy of different settings during mechanical ventilation, such as a higher level of positive end-expiratory pressure (PEEP), or a recruitment maneuver, this approach allows us to evaluate the modification of a lung compartment, such as the nonaerated (i.e., the gasless tissue) or the normally aerated lung compartments, after having applied the "maneuver." These effects will be quantified as a difference between a baseline or pretreatment status, and the new or posttreatment status.

"Tissue Volume" or "Tissue Weight"?

The usefulness of the lung compartment approach in investigating the pathophysiology of acute lung injury (ALI) has become evident within the past decade, as shown by the broad application of lung CT scans by many groups of investigators.[8,9,11,21–25] Unfortunately, when considering the available literature, some differences in the technique used and the analysis performed may affect the comparison of the findings and may result in misinterpretations of the observed results. One of the most important issues not well understood has been the use of the "tissue weight," rather than the "tissue volume," when looking at the lung compartments with different degrees of aeration. If we consider the lung parenchyma as a mixture of gas and tissue, the use of "tissue volume" for the quantification, for instance, of the normally aerated lung compartment will include the amount of tissue that is normally aerated plus the amount of gas that fills the alveoli of this compartment, and is calculated based on the frequency distribution of the CT numbers and the total volume of a lung CT area as follows:

$$Normally\ aerated\ volume = Total\ volume_{area} \times \left[\frac{voxels(-900\ to\ -500\ HU)_{area}}{total\ number\ of\ voxels_{area}}\right]$$

where the $Total\ volume_{area}$ denotes the total lung volume of the area analyzed, the $voxels\ (-900\ to\ -500\ HU)_{area}$ denotes the number of voxels normally aerated (with a CT number between −900 and −500 HU), and the $total\ number\ of\ voxels_{area}$ denotes the total number of voxels included in the lung area analyzed. The same formula applies to each lung compartment. In contrast, to give the right role to this compartment within the functional anatomy of the overall lung parenchyma, we need to focus only on the amount of tissue that is normally

aerated (i.e., the weight of the lung tissue included in this lung compartment):

$$Normally\ aerated\ tissue\ weight = NOR\ volume_{area} \times \left\{1 - \left[\frac{mean\ CT(-900\ to\ -500\ HU)_{area}}{-1000}\right]\right\}$$

where the $NOR\ volume_{area}$ denotes the normally aerated lung volume of the area analyzed and $mean\ CT\ (-900\ to\ -500\ HU)_{area}$ denotes the mean CT number of the overall normally aerated compartment. A numerical example may clarify this point. Let's assume that in a patient with ARDS the volume of the normally aerated compartment at end expiration with a PEEP of 5 cm H_2O is 250 mL, with a mean density of −650 HU, corresponding therefore to 87.5 g of normally aerated lung tissue. After increasing PEEP to 15 cmH_2O, the normally aerated lung volume will increase, for instance, up to 350 mL, with a mean density of −750 HU. This value will correspond to an amount of normally aerated lung tissue of 87.5 g, exactly the same amount recorded at baseline condition. Thus, if we do not correctly consider the real amount of tissue, we will erroneously conclude that increasing PEEP in this particular patient may be effective in improving the normally aerated lung compartment, and thus inferring erroneous information on gas exchange or respiratory mechanics, while indeed there is no real gain in normally aerated lung tissue. The same reasoning may be applied for the poorly aerated and hyperinflated lung compartments. Fortunately, this confusion may not be valid for the nonaerated lung compartment, the gasless tissue, in which the tissue volume and tissue weight usually coincide because there is almost no gas left in this compartment.

Static versus Dynamic CT Scan Imaging

Since the beginning of its application in studying ARDS patients, attention has been paid to the ventilatory setting employed while performing CT scanning. In particular, one of the most important settings has been the use of an end-expiratory or and end-inspiratory pause during the scanning. The maintenance of the respiratory system in a static condition, as during a respiratory pause, provides a good accuracy, for which subsequent quantitative analyses can be performed. If patients breathe during the CT scanning, as occurs in spontaneously breathing patients, the quantification of the gas volume included into the lung parenchyma, and its division in compartments with different degrees of aeration, will inevitably represent an average of the modifications occurring within the lung parenchyma during the tidal breath. In contrast, by keeping the respiratory system in a static condition, we can assure a more precise quantification of its functional anatomy both at end-expiration and at end-inspiration (by applying, respectively, an end-expiratory and end-inspiratory pause). Consequently, the modifications occurring during the tidal breath may be estimated by considering the differences between the functional anatomy at end-expiration and at end-inspiration. This approach has been successfully applied in the study of many different ventilatory strategies, such as the lung distribution of ventilation and its modifications with PEEP,[26] the intratidal lung recruitment,[26] the effects of PEEP,[7,26,27] and the overall lung recruitability.[15] The reason for this approach relies also on the technical characteristics of the first CT scanner available at the time of the first introduction of CT in the study of ARDS, especially in the speed of image acquisition.[16]

In recent years, the introduction of the electron beam CT and new multidetector helical scanners has partially overcome this limitation, providing higher speed for image acquisition. Based on the possibility of acquiring CT images at a subsecond speed (50 to 500 msec) in a quasi-continuous fashion, CT scanning may be used in dynamic conditions, including analysis of mechanical ventilation, and lung perfusion.[13,14] In experimental settings, Markstaller and colleagues used dynamic CT to investigate the variations of functional anatomy and its correlation with the gas exchange during tidal breathing, without interrupting mechanical ventilation.[11,12,28] Most findings reported have been limited to static conditions; this approach, in contrast, may have value in elucidating the dynamics of mechanical ventilation in ARDS patients. As an example, the same group of investigators investigated the pulmonary distribution of time constants during mechanical ventilation, both in healthy and in injured lungs, observing two different patterns of time constant distributions, a discrete one in healthy lungs and a continuous one in ARDS lungs.[29]

Another application of dynamic CT scanning is to study lung perfusion, which has been for many years the "holy grail" of lung research with regard to the pathophysiology of the respiratory system. In fact, if, for studying and visualizing the "ventilatory side" and its regional distribution within the lung parenchyma, CT scanning may be considered a gold standard, no comparable technique, in terms of quantification and precision, has been available for many years to study the "perfusion side" of the lung. Together with positron emission tomographic (PET) scanning, the application of dynamic CT is promising. Although not yet applied in ARDS patients, Jones and colleagues employed dynamic CT to study the effect of body positioning[13] and the effect of hypoxia and inhalation of nitric oxide[14] on the regional distribution of lung perfusion. Although not without technical limitations, such as the possibility of studying only lung slices rather than the whole lung, with the consequent presence of "shift volume effect,"

and the use of contrast material, dynamic CT is a potentially useful technique to better understand the pathophysiology of lung perfusion.

PATHOPHYSIOLOGICAL INSIGHTS—ARDS MODELING

Before its application in ARDS patients, CT had begun to gain popularity for studying the development of lung atelectasis during anesthesia and paralysis.[30] When CT was first applied in ARDS patients, findings were unexpected. In contrast to previous theories, ARDS was not a homogeneous disease but was quite uneven, with a proclivity for the most dependent lung regions; the nondependent areas were relatively spared[4,5] (Fig. 1). From that first observation, CT has provided several findings that over time have changed our view of ARDS.[31]

From the "Stiff Lung" to the "Baby Lung"

During the first decade after the identification of ARDS, the lung parenchyma affected by this syndrome was considered as a "stiff lung."[1] This conclusion was drawn by the observation of a very low compliance of the respiratory system, associated with the radiological and histopathological findings of diffuse alveolar infiltrates. This conceptual approach to ARDS lung unfortunately led physicians to use high tidal volumes (12 to 15 mL/kg) and airway pressures, during mechanical ventilation, aimed at opposing the great "stiffness" of the lung to improve oxygenation. As Pontoppidan and colleagues reported in their manuscript, "we ventilated thousands of patients in this way, and the only side effect was hypocapnia."[2] Indeed, besides the common finding of hypocapnia, the real detrimental effect of such a ventilatory approach was the occurrence of barotrauma. The first CT scan performed on a patient affected by ARDS revealed a quite different picture on an axial lung image: rather than homogeneous, the disease affected the lung parenchyma in an uneven pattern. Three different zones may be recognized: a near-normal area in the nondependent lung regions (i.e., the parasternal regions while in supine position), a ground-glass opacification in the middle lung regions, and a consolidated area in the most dependent lung regions (i.e., the paravertebral regions while in the supine position). The subsequent quantitative analysis of CT images revealed that the near-normal areas localized in the nondependent lung regions was normally aerated lung tissue, but the quantity of this lung compartment was markedly reduced (~200 to 300 g) as compared with a normal subject (~700 g). This observation led to the concept of the "baby lung" rather than the "stiff lung"; the lung affected by ARDS is small, with a normal portion having the dimension of the lung of a 5- to 6-year-old child. What was surprising at the beginning was the discovery that, as a consequence of such a functional morphology, the compliance of the respiratory system was strictly correlated not with the amount of lung atelectasis (i.e., the nonaerated lung tissue), but rather, with the amount of normal lung (i.e., the normally aerated lung tissue).[20] These findings gradually changed our view of ARDS and in particular our view of how to ventilate such patients. Given the functional morphology of ARDS lung as observed, it becomes evident that the application of very high tidal volume to a very small lung, as commonly used during these years, will generate extremely high pressures and wall stresses that will lead to tissue rupture (i.e., barotrauma). This leads to the concept of a more "gentle" ventilatory treatment of the lung. Thereafter, first with the introduction of extracorporeal support,[32] and later with the introduction of a low tidal volume ventilation and permissive hypercapnia,[33] the concept of a gentle ventilatory treatment of the ARDS has gained acceptance.

From the "Baby Lung" to the "Sponge Lung"

The baby lung was initially thought to be an anatomical entity, usually located in the nondependent lung regions. This conceptual framework was originally the premise for the proposal of prone positioning in ARDS patients. It was hypothesized that by turning the patient in a prone position, the baby lung, once located in the dependent lung regions after the change of position, would have been more perfused because lung perfusion is gravity dependent.[34] Thus the possibility of improving systemic oxygenation was at hand. Surprisingly, although systemic oxygenation did actually improve in most patients, we consistently observed a redistribution of the lung densities (i.e., lung atelectasis and/or consolidations), from the most dependent lung regions, the paravertebral areas in the supine position, to the most dependent lung regions in the prone position (i.e., the parasternal lung areas).[34,35] In an attempt to understand the mechanisms underlying the redistribution of lung densities with prone position, a quantitative analysis of the regional distribution of CT scan variables was performed. From this analysis it appeared that the pulmonary edema, as estimated by the excess tissue mass,[36] accumulates within the lung parenchyma according to an even pattern along the sternovertebral gradient, and it is not distributed according to gravitational forces,[37] as previously observed in both experimental and clinical settings.[38,39] Therefore, if homogeneously distributed within the lung parenchyma, how can lung edema generate the baby lung aspect? A novel model of ARDS physiopathology was proposed: the "sponge lung".[40] According to this view, lung edema formation affects the whole lung in an even

distribution, but, due to the increased lung weight caused by edema, in the presence of gravitational forces, the increased mass will generate lung collapse in the most dependent lung regions, where the excess tissue weight is greater. As a consequence, the increased lung weight, while collapsing the most dependent lung regions, will squeeze out the gas volume originally filling this portion of the lung from the most dependent to the nondependent lung regions, leading to the classical appearance of lung parenchyma on CT scan images. From this point of view, the lung affected by ARDS may be considered as a sponge full of water: as long as the sponge is immersed in water, with almost no influence of the gravitational field, the water absorbed by the sponge will be evenly distributed within it; in contrast, when the sponge is pulled out of the water, the liquid absorbed by the sponge will tend to distribute in the most dependent regions due to the gravitational forces and the consequent increased weight of the nondependent regions onto the dependent ones. The final results will be the presence of "sponge atelectasis" in the most dependent portion of the sponge. Once again, the use of the quantitative analysis on CT provided the possibility to quantify the gravitational forces causing lung collapse in the most dependent lung regions, called "superimposed pressure".[35,37] At each level of the lung along the sternovertebral axis, the weight of the tissue above such a level will generate a pressure (the superimposed pressure) that will determine alveolar collapse in that level and that will depend on the height of tissue above the level and the fraction of lung tissue included in the portion of the lung above that level:

$$Superimposed\ pressure_{level} = height_{level} \times \left[1 - \left(\frac{mean\ CT_{level}}{-1000}\right)\right] + superimposed\ pressure_{above}$$

where $height_{level}$ denotes the height of the given lung level; $mean\ CT_{level}$ the mean density, expressed in CT number, of the given lung level; and $superimposed\ pressure_{above}$ denotes the superimposed pressure of the portion of lung parenchyma above the given level.

The "Recruitable Lung" and the "Consolidated Lung": A Novel View

Novel findings recently observed in a quite large population of patients affected by ALI or ARDS may add further insights to ARDS lung modeling.[15] It has been well known since its first identification that ARDS is characterized by alveolar collapse. As a consequence, ventilatory strategies aimed at opening the lung, such as the initial application of PEEP,[41] or later on, the use of recruitment maneuvers,[42–44] gained favor until the introduction of the "open lung approach."[45] The importance of lung recruitment is well accepted in treatment of ARDS patients, but the mechanisms underlying its pathophysiology have not yet been elucidated. Much of the data regarding the "rules" of lung recruitment were derived from experimental models of ARDS, in which most of the time the maximal amount of the potential for lung recruitment is greater than that observed in patients. Moreover, response to recruitment maneuvers varies considerably among different ARDS patients. To gain insights into the phenomenon, we designed a study to examine the maximal potential for lung recruitment (as detected by CT), in a large population affected by ALI/ARDS.[15] Sixty-eight patients were enrolled from four institutions; whole-lung CT scans were performed during an end-expiratory pause at a PEEP of 5 cm H_2O, and during an end-inspiratory pause at a plateau pressure of 45 cm H_2O. The potential for lung recruitment was defined as the difference in nonaerated lung tissue (i.e., the gasless portion of lung parenchyma) between the two levels of airway pressures, and was expressed as a fraction of the total lung weight. We found that lung recruitment varied widely among the study population: the maximal lung recruitability varied from a quite negligible fraction to a more than 50% fraction of the total lung weight (Fig. 3). Surprisingly, CT revealed an unexpected finding: the amount of the consolidated lung tissue (i.e., the amount of gasless tissue not recruitable even applying 45 cm H_2O airway pressure), was constant throughout the population, corresponding to ~24% of the total lung tissue weight. It followed a strict association between the maximal lung recruitability and the total amount of nonaerated lung tissue at baseline (i.e., the gasless tissue). In other words, the greater the maximal potential for lung recruitment, the greater was the overall severity of lung injury at baseline, as detected by the amount of gasless tissue, and confirmed by the analysis of gas exchange and respiratory mechanics. Patients with a higher amount of potential for lung recruitment exhibited a higher mortality rate at discharge from intensive care units, as compared with patients with a lower amount of potential for lung recruitment. A novel view of ARDS lung may be derived from these observations. When ARDS affects the lung parenchyma, the extent of the inflammatory reaction deriving from the initial insult will affect the development of lung edema, and therefore the development of gravity-dependent alveolar collapse (i.e., the potential for lung recruitment). It is conceivable that the consolidated lung tissue constantly observed reflects the "core disease" of ARDS, whereas the associated collapsed and therefore recruitable lung tissue may reflect the extent of the surrounding inflammatory reaction, which will vary among patients and will be related to the severity of the disease and

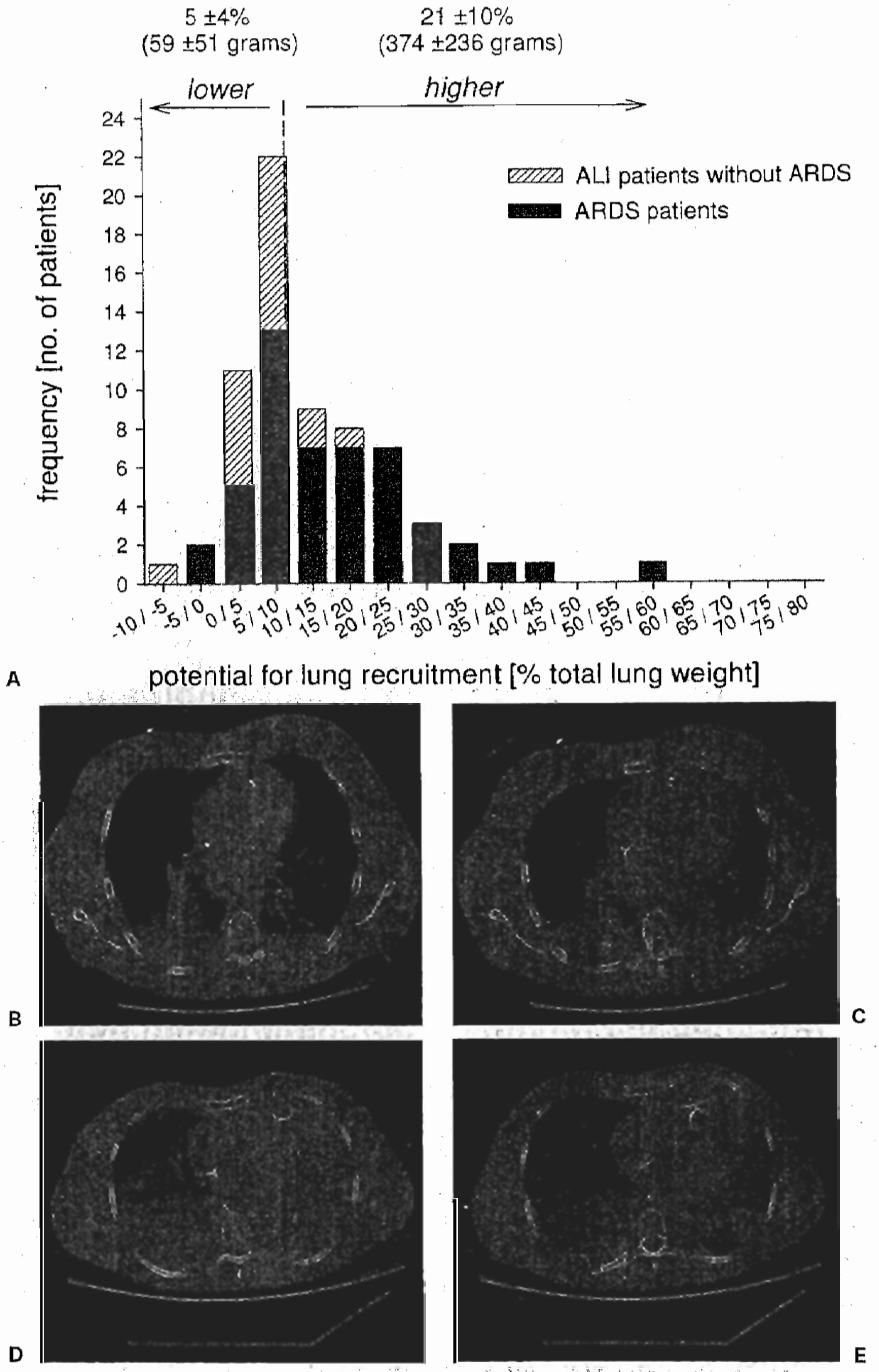

Figure 3 (A) Frequency distribution of acute lung injury/acute respiratory distress syndrome (ALI/ARDS) patients according to the potential for lung recruitment, and (B,C) representative lung computed tomographic (CT) images at airway pressures of 5 and 45 cm H_2O from patients with lower and (D,E) higher potential for lung recruitment. The frequency distribution of the overall study population is shown according to the total amount of lung recruitability, expressed as a percentage of the total lung weight (A). ALI without ARDS denotes patients with ALI without ARDS having a PaO_2:FO_2 ratio of < 300 but not < 200. ARDS denotes patients with a PaO_2:FiO_2 ratio of < 200. The overall study population was divided into patients with lower and patients with higher potential for lung recruitment, according to its median value (9% of the total lung weight). (B and C) show representative lung CT slices obtained 2 cm above the diaphragm dome at airway pressures of 5 cm H_2O (B) and 45 cm H_2O (C) from a patient with lower potential for lung recruitment. The amount of the potential for lung recruitment was 4%, and the proportion of the consolidated lung tissue was 33% of the total lung weight. (D and E) show representative lung CT slices obtained 2 cm above the diaphragm dome at airway pressures of 5 cm H_2O (D) and 45 cm H_2O (E) from a patient with higher potential for lung recruitment. The amount of potential for lung recruitment was 37%, whereas the proportion of the consolidated lung tissue was 27% of the total lung weight. From Gattinoni et al,[15] with permission.

therefore mortality. The sponge lung may thus be considered as made of two different portions: a core not-recruitable nucleus and a collapsed and recruitable portion.

CLINICAL INSIGHTS

The wide use of CT by different groups of investigators and the results obtained in the past decade have led to the incorporation of CT in the clinical ventilatory management of ARDS patients. Recent improvements have been made in understanding the meaning of the pressure–volume (PV) curve of the respiratory system and its utility in setting mechanical ventilation. In contrast to what had been thought, lung recruitment appeared to be a continuous phenomenon occurring along the entire PV curve,[7,27] starting at the lower inflection point of the curve.[8] In contrast, lung derecruitment was significant only at airway pressures below the maximal point of curvature of the deflation limb, which has been suggested as a useful tool for setting PEEP.[9] Although not yet investigated in clinical settings, CT has revealed an important and probably unexpected role of intra-abdominal pressure in the development of lung edema during experimental ARDS.[10] The higher the intra-abdominal pressure while the lung parenchyma is already injured, the greater will be the accumulation of lung edema, as detected by the excess tissue mass. Here, for the sake of brevity, we will focus our attention on the most recent data obtained in a relatively large population of ARDS patients on lung recruitment because they may substantially affect our clinical ventilatory strategies.

PEEP Setting and Potential for Lung Recruitment

As mentioned earlier, lung recruitment has been acknowledged as a key issue in the ventilatory management of ARDS. The importance of lung recruitment led in the early 1990s to novel ventilatory strategies (i.e., the open lung approach[45] or lung protective strategy[42]). This ventilatory strategy included the use of a recruitment maneuver to open the lung, and the use of a high level of PEEP and low tidal volumes to keep the lung open, avoiding both the regional and the global stress and strain on the lung parenchyma. Fortunately, this approach showed benefit, as compared with the traditional ventilatory strategies, with improved survival[42,46] and attenuation of the inflammatory reaction of the lung.[47] Similarly, ventilation at low tidal volume alone was shown to be effective in reducing the mortality among patients with ALI or ARDS.[48] In contrast, as shown in the recent NIH-ALVEOLI study,[49] the addition of high levels of PEEP to low tidal volume ventilation did not further decrease the mortality of these patients, as compared with lower PEEP levels.

From these data, some observations are pivotal. The beneficial effects of adding PEEP in terms of reduction of lung atelectasis and decreasing global and regional alveolar stress and strain were mainly studied in animal models of ALI, characterized by a large amount of collapsed, and therefore recruitable, lung tissue.[27,50,51] In human ARDS, however, some patients demonstrate a minimal response to ventilator procedures aimed at recruiting collapsed lung regions, suggesting their maximal potential for lung recruitment may be low. Moreover, ARDS patients may differ substantially in terms of response to recruitment maneuvers: some show a good response to ventilatory maneuvers, whereas others do not.[43,49,52] It is conceivable that the application of a high level of PEEP in patients with low lung recruitability may be harmful. In fact, the application of such a PEEP level will only determine an increase in lung inflation of the already-open portions of the lung, with no beneficial effects with regard to the reduction of alveolar stress and strain because only a negligible fraction of the lung is recruitable. Therefore, if patients with lower or higher lung recruitability are randomly assigned to lower or higher PEEP levels, a strategy employed in the NIH-ALVEOLI study,[49] the possible benefits of higher PEEP levels in patients with higher lung recruitability may be offset by the harmful effects caused by high PEEP levels in patients with lower lung recruitability. We consequently hypothesized that the knowledge of the maximal capacity of the lung to be recruited (i.e., the potential for lung recruitment), might determine the response to PEEP.[15] The maximal potential for lung recruitment, as well as the lung functional anatomy at two different PEEP levels (5 and 15 cm H_2O), was estimated in 68 patients with ALI/ARDS by using CT as the gold standard measurement of lung recruitment.[16] As mentioned earlier, a large variation in the overall population was observed with regard to the frequency distribution of the potential for lung recruitment, which ranged from –9 to 59% of the total lung weight, with a mean value of $13 \pm 11\%$, corresponding to an absolute weight of 217 ± 232 g (Fig. 3). Moreover, the response to higher PEEP in terms of lung recruitment was strongly associated with the maximal potential for lung recruitment: the higher is the maximal lung recruitability, the higher will be the amount of collapsed lung tissue that PEEP can maintain recruited (Fig. 4). In fact, the application of 15 cm H_2O PEEP was able to consistently maintain recruited about ~50% of the potential for lung recruitment, irrespective of its absolute amount.

From these data, one point is critical: the assessment of lung recruitability should be a prerequisite for a rational setting of PEEP. In fact, the application of high PEEP levels in a patient with low lung recruitability may only maintain recruited lung regions that are already aerated, leading to overdistension, whereas collapsed lung tissue cannot be inflated because the

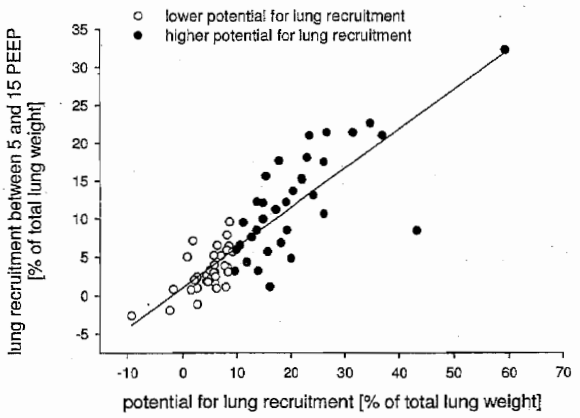

Figure 4 Lung recruitment induced by increasing positive end-expiratory pressure (PEEP) from 5 to 15 cm H_2O as a function of the potential for lung recruitment. Lung recruitment induced by PEEP was calculated as the decrease in nonaerated lung tissue between 5 and 15 cm H_2O. Both variables are expressed as a proportion of the total lung weight measured at baseline PEEP of 5 cm H_2O ($r^2 = 0.72$, $p < 0.001$, slope = 0.52, y intercept = 1.03). From Gattinoni et al,[15] with permission.

lung recruitability in such patients is negligible. In this setting, high PEEP levels may be detrimental. In contrast, the application of low PEEP levels in a patient with high lung recruitability may be insufficient because a large fraction of the collapsed lung tissue will collapse at end-expiration, and will undergo cycling intra-tidal collapse and de-collapse between inspiration and expiration. In these patients, high PEEP levels may be beneficial by preventing alveolar collapse at end-expiration, and by preventing alveolar intra-tidal collapse and de-collapse. On the basis of this concept, we limit PEEP levels in patients with low lung recruitability (< 10 cm H_2O), whereas we apply high PEEP levels (> 15 cm H_2O) in patients with high lung recruitability. However, a randomized clinical trial is needed to determine whether high PEEP (as compared with low PEEP) affects outcomes among ARDS patients with a higher potential for lung recruitment.

ARDS Definition

During the last 3 decades, it has been progressively recognized that, irrespective of the initial insult, ARDS is characterized by altered permeability of the alveolar-capillary membrane, with the formation of high-permeability lung edema, the pathognomonic lesion of the syndrome. However, this alteration was never directly included in the definition of ARDS. After the first characterization of ARDS by Ashbaugh and colleagues as a syndrome showing "acute onset of tachypnea, hypoxemia, and loss of compliance,"[1] not responding to the ordinary methods of respiratory therapy, Murray and colleagues proposed a lung injury score for ARDS definition.[53] This score included a progressively decreasing ratio of arterial partial pressure of oxygen (PaO_2) on inspired oxygen fraction (FiO_2), different degrees of consolidation on the chest radiograph, and a progressively decreased compliance of the respiratory system. The most widely accepted and employed definition of ARDS was proposed by the American-European Consensus Conference, which relies primarily on hypoxemia (PaO_2:FiO_2 < 300) and the presence of bilateral infiltrates (by conventional chest radiographs), in the absence of left atrial hypertension.[54] Although not substantially different, a new definition, developed by using the Delphi technique, was recently proposed[55,56] that included systemic hypoxemia (PaO_2:FiO_2 ratio < 200 at a PEEP ≥ 10 cm H_2O), and bilateral pulmonary infiltrates by chest radiographs.

All the current definitions to identify ARDS include the presence of bilateral pulmonary infiltrates (by chest radiographs), which is thought to be a surrogate for high-permeability lung edema. Unfortunately, chest radiographic "infiltrates" may be the morphological sign of myriad conditions, such as lung atelectasis, consolidation, interstitial edema, intra-alveolar flooding or consolidation, and the like.[16] Therefore, although chest radiographs are a hallmark feature of ARDS, they are nonspecific. In contrast, CT may be a much better tool to detect lung edema formation, especially by applying to CT images a quantitative analysis, thereby evaluating the excess tissue mass.[36] In the investigation mentioned earlier, which consisted of 68 patients with ALI or ARDS (according to the American-European Consensus Conference criteria), we also examined 34 control patients with unilateral pneumonia and 39 controls with healthy lungs who underwent whole-lung CT for diagnostic purposes.[15] By looking at the total lung tissue weight, which approximately reflects the amount of inflammatory edema, we observed that patients with ALI/ARDS had significantly greater lung tissue weight (~1500 g) than patients with either healthy lungs or unilateral pneumonia (respectively, ~850 and 1200 g). However, when dividing the overall ALI/ARDS population according to the maximal lung recruitability of each patient, it appeared that the difference in lung tissue weight between ALI/ARDS patients and patients with unilateral pneumonia was mainly due to the ALI/ARDS patients with a higher potential for lung recruitment (with a lung tissue weight of ~1700 g). In fact, the lung tissue weight of ALI/ARDS patients with a lower potential for lung recruitment was similar to that observed in patients with unilateral pneumonia (~1250 g). The same picture applies for the amount of nonaerated lung tissue (i.e., the gasless tissue).

In our opinion, these findings highlight the importance of considering the hallmark sign, of ARDS (i.e., high-permeability lung edema), in its definition, as previously suggested.[57,58] From this point of view, it is surprising that in about half of the patients currently

considered as affected by ALI/ARDS, as defined by the American-European Consensus Conference, the amount of collapsed lung tissue (the potential for lung recruitment), which is strictly related to the formation of gravity-dependent lung edema, is almost negligible and similar to patients with unilateral pneumonia who are not included in the ALI/ARDS definition. Although not sufficient to propose a novel definition of ALI/ARDS, our data suggest that measurement of a threshold value of lung edema should be considered to correctly define this syndrome as a specific entity. Surprisingly, similar arguments were discussed ~10 years ago[57,58] but did not lead to a modification of ARDS definition. One explanation of this gap reflects the difficulty in measuring either lung edema or the permeability of the alveolar-capillary membrane. Although not yet broadly employed, and not always feasible in the clinical setting, CT may provide a reasonable tool to estimate lung edema with acceptable precision. We should not be surprised if in 5 or 10 years, along with improvements in CT technology, CT will play an important and integral role in the clinical care of patients with ALI and ARDS.

REFERENCES

1. Ashbaugh DG, Bigelow DB, Petty TL, Levine BE. Acute respiratory distress in adults. Lancet 1967;2:319–323
2. Pontoppidan H, Geffin B, Lowenstein E. Acute respiratory failure in the adult, III. N Engl J Med 1972;287:799–806
3. Rommelsheim K, Lackner K, Westhofen P, Distelmaier W, Hirt S. Respiratory distress syndrome of the adult in the computer tomograph [in German]. Anasth Intensivther Notfallmed 1983;18:59–64
4. Gattinoni L, Mascheroni D, Torresin A, et al. Morphological response to positive end expiratory pressure in acute respiratory failure: computerized tomography study. Intensive Care Med 1986;12:137–142
5. Maunder RJ, Shuman WP, McHugh JW, Marglin SI, Butler J. Preservation of normal lung regions in the adult respiratory distress syndrome: analysis by computed tomography. JAMA 1986;255:2463–2465
6. Gattinoni L, Presenti A, Torresin A, et al. Adult respiratory distress syndrome profiles by computed tomography. J Thorac Imaging 1986;1:25–30
7. Crotti S, Mascheroni D, Caironi P, et al. Recruitment and derecruitment during acute respiratory failure: a clinical study. Am J Respir Crit Care Med 2001;164:131–140
8. Downie JM, Nam AJ, Simon BA. Pressure–volume curve does not predict steady-state lung volume in canine lavage lung injury. Am J Respir Crit Care Med 2004;169:957–962
9. Albaiceta GM, Taboada F, Parra D, et al. Tomographic study of the inflection points of the pressure–volume curve in acute lung injury. Am J Respir Crit Care Med 2004;170:1066–1072
10. Quintel M, Pelosi P, Caironi P, et al. An increase of abdominal pressure increases pulmonary edema in oleic acid–induced lung injury. Am J Respir Crit Care Med 2004;169:534–541
11. Markstaller K, Eberle B, Kauczor HU, et al. Temporal dynamics of lung aeration determined by dynamic CT in a porcine model of ARDS. Br J Anaesth 2001;87:459–468
12. Markstaller K, Kauczor HU, Weiler N, et al. Lung density distribution in dynamic CT correlates with oxygenation in ventilated pigs with lavage ARDS. Br J Anaesth 2003;91:699–708
13. Jones AT, Hansell DM, Evans TW. Pulmonary perfusion in supine and prone positions: an electron-beam computed tomography study. J Appl Physiol 2001;90:1342–1348
14. Jones AT, Hansell DM, Evans TW. Pulmonary perfusion quantified by electron-beam computed tomography: effects of hypoxia and inhaled NO. Eur Respir J 2003;21:855–861
15. Gattinoni L, Caironi P, Cressoni M, et al. Lung recruitment in patients with the acute respiratory distress syndrome. N Engl J Med 2006;354:1775–1786
16. Gattinoni L, Caironi P, Pelosi P, Goodman LR. What has computed tomography taught us about the acute respiratory distress syndrome? Am J Respir Crit Care Med 2001;164:1701–1711
17. Mull RT. Mass estimates by computed tomography: physical density from CT numbers. AJR Am J Roentgenol 1984; 143:1101–1104
18. Geise RA, McCullough EC. The use of CT scanners in megavoltage photon-beam therapy planning. Radiology 1977;124:133–141
19. Phelps ME, Gado MH, Hoffman EJ. Correlation of effective atomic number and electron density with attenuation coefficients measured with polychromatic x rays. Radiology 1975;117(3 Pt 1):585–588
20. Gattinoni L, Pesenti A, Avalli L, Rossi F, Bombino M. Pressure–volume curve of total respiratory system in acute respiratory failure: computed tomographic scan study. Am Rev Respir Dis 1987;136:730–736
21. Rouby JJ, Puybasset L, Nieszkowska A, Lu Q. Acute respiratory distress syndrome: lessons from computed tomography of the whole lung. Crit Care Med 2003;31(Suppl 4):S285–S295
22. Luecke T, Roth H, Joachim A, et al. Effects of end-inspiratory and end-expiratory pressures on alveolar recruitment and derecruitment in saline-washout-induced lung injury: a computed tomography study. Acta Anaesthesiol Scand 2004;48:82–92
23. Grasso S, Terragni P, Mascia L, et al. Airway pressure-time curve profile (stress index) detects tidal recruitment/hyperinflation in experimental acute lung injury. Crit Care Med 2004;32:1018–1027
24. Patroniti N, Bellani G, Manfio A, et al. Lung volume in mechanically ventilated patients: measurement by simplified helium dilution compared to quantitative CT scan. Intensive Care Med 2004;30:282–289
25. Luecke T, Herrmann P, Kraincuk P, Pelosi P. Computed tomography scan assessment of lung volume and recruitment during high-frequency oscillatory ventilation. Crit Care Med 2005;33(Suppl 3):S155–S162
26. Gattinoni L, Pelosi P, Crotti S, Valenza F. Effects of positive end-expiratory pressure on regional distribution of tidal volume and recruitment in adult respiratory distress syndrome. Am J Respir Crit Care Med 1995;151:1807–1814
27. Pelosi P, Goldner M, McKibben A, et al. Recruitment and derecruitment during acute respiratory failure: an experimental study. Am J Respir Crit Care Med 2001;164:122–130

28. David M, Karmrodt J, Bletz C, et al. Analysis of atelectasis, ventilated, and hyperinflated lung during mechanical ventilation by dynamic CT. Chest 2005;128: 3757–3770
29. Doebrich M, Markstaller K, Karmrodt J, et al. Analysis of discrete and continuous distributions of ventilatory time constants from dynamic computed tomography. Phys Med Biol 2005;50:1659–1673
30. Brismar B, Hedenstierna G, Lundquist H, Strandberg A, Svensson L, Tokics L. Pulmonary densities during anesthesia with muscular relaxation: a proposal of atelectasis. Anesthesiology 1985;62:422–428
31. Gattinoni L, Pesenti A. The concept of "baby lung." Intensive Care Med 2005;31:776–784
32. Gattinoni L, Pesenti A, Bombino M, Pelosi P, Brazzi L. Role of extracorporeal circulation in adult respiratory distress syndrome management. New Horiz 1993;1:603–612
33. Hickling KG, Walsh J, Henderson S, Jackson R. Low mortality rate in adult respiratory distress syndrome using low-volume, pressure-limited ventilation with permissive hypercapnia: a prospective study. Crit Care Med 1994;22: 1568–1578
34. Langer M, Mascheroni D, Marcolin R, Gattinoni L. The prone position in ARDS patients: a clinical study. Chest 1988;94:103–107
35. Gattinoni L, Pelosi P, Vitale G, Pesenti A, D'Andrea L, Mascheroni D. Body position changes redistribute lung computed-tomographic density in patients with acute respiratory failure. Anesthesiology 1991;74:15–23
36. Gattinoni L, Pesenti A, Bombino M, et al. Relationships between lung computed tomographic density, gas exchange, and PEEP in acute respiratory failure. Anesthesiology 1988; 69:824–832
37. Pelosi P, D'Andrea L, Vitale G, Pesenti A, Gattinoni L. Vertical gradient of regional lung inflation in adult respiratory distress syndrome. Am J Respir Crit Care Med 1994;149:8–13
38. Jones T, Jones HA, Rhodes CG, Buckingham PD, Hughes JM. Distribution of extravascular fluid volumes in isolated perfused lungs measured with H215O. J Clin Invest 1976; 57:706–713
39. Hales CA, Kanarek DJ, Ahluwalia B, et al. Regional edema formation in isolated perfused dog lungs. Circ Res 1981;48:121–127
40. Bone RC. The ARDS lung: new insights from computed tomography. JAMA 1993;269:2134–2135
41. Falke KJ, Pontoppidan H, Kumar A, Leith DE, Geffin B, Laver MB. Ventilation with end-expiratory pressure in acute lung disease. J Clin Invest 1972;51:2315–2323
42. Amato MB, Barbas CS, Medeiros DM, et al. Effect of a protective-ventilation strategy on mortality in the acute respiratory distress syndrome. N Engl J Med 1998;338: 347–354
43. Villagra A, Ochagavia A, Vatua S, et al. Recruitment maneuvers during lung protective ventilation in acute respiratory distress syndrome. Am J Respir Crit Care Med 2002;165:165–170
44. Brower RG, Morris A, MacIntyre N, et al. Effects of recruitment maneuvers in patients with acute lung injury and acute respiratory distress syndrome ventilated with high positive end-expiratory pressure. Crit Care Med 2003;31: 2592–2597
45. Lachmann B. Open up the lung and keep the lung open. Intensive Care Med 1992;18:319–321
46. Villar J, Kacmarek RM, Perez-Mendez L, Aguirre-Jaime A. A high positive end-expiratory pressure, low tidal volume ventilatory strategy improves outcome in persistent acute respiratory distress syndrome: a randomized, controlled trial. Crit Care Med 2006;34:1311–1318
47. Ranieri VM, Suter PM, Tortorella C, et al. Effect of mechanical ventilation on inflammatory mediators in patients with acute respiratory distress syndrome: a randomized controlled trial. JAMA 1999;282:54–61
48. Ventilation with lower tidal volumes as compared with traditional tidal volumes for acute lung injury and the acute respiratory distress syndrome. The Acute Respiratory Distress Syndrome Network. N Engl J Med 2000;342:1301–1308
49. Brower RG, Lanken PN, MacIntyre N, et al. Higher versus lower positive end-expiratory pressures in patients with the acute respiratory distress syndrome. N Engl J Med 2004; 351: 327–336
50. Kloot TE, Blanch L, Melynne YA, et al. Recruitment maneuvers in three experimental models of acute lung injury: effect on lung volume and gas exchange. Am J Respir Crit Care Med 2000;161:1485–1494
51. Lim SC, Adams AB, Simonson DA, et al. Intercomparison of recruitment maneuver efficacy in three models of acute lung injury. Crit Care Med 2004;32:2371–2377
52. Gattinoni L, Pelosi P, Suter PM, Pedoto A, Vercesi P, Lissoni A. Acute respiratory distress syndrome caused by pulmonary and extrapulmonary disease: different syndromes? Am J Respir Crit Care Med 1998;158:3–11
53. Murray JF, Matthay MA, Luce JM, Flick MR. An expanded definition of the adult respiratory distress syndrome. Am Rev Respir Dis 1988;138:720–723
54. Bernard GR, Artigas A, Brigham KL, et al. The American-European Consensus Conference on ARDS: definitions, mechanisms, relevant outcomes, and clinical trial coordination. Am J Respir Crit Care Med 1994;149(3 Pt 1):818–824
55. Fink A, Kosecoff J, Chassin M, Brook RH. Consensus methods: characteristics and guidelines for use. Am J Public Health 1984;74:979–983
56. Ferguson ND, Davis AM, Slutsky AS, Stewart TE. Development of a clinical definition for acute respiratory distress syndrome using the Delphi technique. J Crit Care 2005;20:147–154
57. Schuster DP. What is acute lung injury? What is ARDS? Chest 1995;107:1721–1726
58. Schuster DP. Identifying patients with ARDS: time for a different approach. Intensive Care Med 1997;23:1197–1203